ISSN 1819-7140, Russian Journal of Pacific Geology, 2011, Vol. 5, No. 2, pp. 111–128. © Pleiades Publishing, Ltd., 2011.
Original Russian Text © A.V. Koloskov, 2011, published in Tikhookeanskaya Geologiya, 2011, Vol. 30, No. 2, pp. 27–45.

Petrological–Geochemical Features of the Cretaceous and Cenozoic Intrusive Magmatism of Kamchatka, the Melt Sources, and the Geodynamic Settings

A. V. Koloskov

Institute of Volcanology and Seismology, Far East Branch, Russian Academy of Sciences, bul'v. Piipa 9, Petropavlovsk-Kamchatskii, 683006 Russia

E-mail: kolosav@ksnet.ru

Received April 4, 2010

Abstract—A comparative analysis of the geological setting and composition was carried out for the Cretaceous, Eocene, and Miocene–Pliocene granitoids of Kamchatka. New petrochemical, geochemical, and isotope data are reported. The alkaline granitoids and granites of the Sredinny Range in Kamchatka have an enriched isotope composition and elevated contents of Rb, Th, U, and LREE as compared to their analogs in the eastern part of the region. The largest scale Cretaceous crustal magmatism was formed in a setting of intense tectonic motions and metamorphism. The smaller scale Eocene magmatism produced crustal granitoid melts in the Sredinny Range of Kamchatka and mantle initially basaltic melts that evolved to granites in the southeastern Kamchatka and Ganalsky Range. These processes were accompanied by the rejuvenated of the older crust and the local formation of a new crust. The low-volume crustal–mantle Miocene–Pliocene magmatism of variable composition was developed in volcanic belts, forming the upper crustal horizons on the existing crystalline basement.

Keywords: *petrochemistry, geochemistry, isotopy, granitoids, magmatism, Mesozoic–Cenozoic, Kamchatka.*

DOI: 10.1134/S1819714011020060

INTRODUCTION

Cretaceous–Cenozoic intrusive rocks were distinguished in Kamchatka during geological surveys (V.A. Yarmolyuk, A.F. Marchenko, M.I. Goryaev, M.M. Lebedev, V.N. Bondarenko, S.E. Aprelkov, and others) and some thematical works as early as the 1960–1970s [3, 5, 19, 23]. In these works, the compositional features of the magmatic rocks were considered in the framework of the formation analysis, which is mainly based on the petrographic description and bulk chemical composition.

The geochemical and isotope compositions of the granitoids remain poorly studied. The problems of the petrogenesis and geodynamic setting of the Cenozoic granitoid magmatism of Kamchatka were mainly considered for the oldest Cretaceous–Paleogene rocks of the Malka Uplift [17].

The comparative consideration of the different-age manifestations of this rock series is of great significance for analyzing the growth and evolution of the continental crust of Kamchatka. The problem whether this crust is newly formed or is ancient in age and existed already in the Proterozoic has been the subject of hot debates at least for half a century [8].

This paper is dedicated to the examination of the structural position of the Kamchatka granitoids, as well as the new age (Table 1), geochemical (Table 2), and isotope (Tables 3, 4) data. Using these data, the geodynamic setting of the granitoids and the main stages of the formation of the continental crust at Kamchatka were determined.

GEOLOGICAL REVIEW

The paper addresses three stages of the granitoid magmatism: the Cretaceous, Eocene, and Miocene–Pliocene.

The Cretaceous granitoids are widely developed in the central part of the Sredinny Range of Kamchatka and on its slopes (the valleys of the Ichi, Krutogorova, Srednyaya Andrianovka, Levyi Kheivan, and Pravaya Kolpakova rivers). All these bodies are confined to the gneiss-granite domes. In works [18, 23], they are united into the Late Cretaceous–Paleogene gabbroplagiogranite formation. According to the geological survey [8], they are ascribed to the Early Cretaceous Krutogorovsky and Late Cretaceous Kol'skii complexes. However, the recent U–Pb zircon dating carried out at the All-Russian Karpinskii Research Institute of Geology (VSEGEI) [8] yielded principally new age data on the Late Cretaceous age (80 ± 5, 81 ± 2.5 Ma) of the granitoids of the Krutogorovsky Massif—the key massif for all the complex. However, it

Table 1. Results of the K–Ar age determinations of the intrusive rocks of Kamchatka

Ordinal no.	Sample no.	Massif	Rock	Potassium, % ± σ	$40Ar_{rad}$ ng/g ± σ	Age, Ma ± 2σ
1	1002	Shipunsky	granodiorite	1.28 ± 0.02	3.997 ± 0.014	44.5 ± 1.4
2	1026	The same	diorite	1.44 ± 0.02	4.068 ± 0.016	40.3 ± 1.2
3	1783	Belaya R.	granite	2.73 ± 0.03	6.94 ± 0.02	36.3 ± 0.8
4	8682	Akhomten	diorite	2.69 ± 0.05	2.546 ± 0.014	13.6 ± 0.5
5	04	The same	granite	2.57 ± 0.03	2.4 ± 0.2	13 ± 1.5
6	2003/2	Kensol R.	granodiorite	1.82 ± 0.02	1.600 ± 0.010	12.6 ± 0.3
7	8626	Akhomten	diorite	4.70 ± 0.05	3.952 ± 0.014	12.1 ± 0.3
8	3704	Kensol R.	granodiorite	1.89 ± 0.02	1.490 ± 0.007	11.3 ± 0.3
9	K-11	Lake Angre	diorite	1.85 ± 0.04	1.391 ± 0.008	10.8 ± 0.5
10	8131/2	Ganalsky	diorite	2.26 ± 0.05	1.347 ± 0.013	8.6 ± 0.4
11	K-116	Barabsky	gabbrodiorite	1.02 ± 0.02	0.577 ± 0.008	8.1 ± 0.4
12	K-47	The same	diorite	1.80 ± 0.02	0.958 ± 0.008	7.7 ± 0.2
13	014273	Avachinsky	granodiorite	2 ± 0.02	0.8 ± 0.2	6 ± 2
14	6278/2	Timonovsky	diorite	1.71 ± 0.03	0.714 ± 0.008	6.0 ± 0.3
15	6231	Avachinsky	diorite	2.11 ± 0.03	0.806 ± 0.012	5.5 ± 0.3
16	3237-66	Syrytsin R.	diorite	2.12 ± 0.03	0.744 ± 0.010	5.0 ± 0.2
17	K-61	Barabsky	granodiorite	2.60 ± 0.03	0.826 ± 0.007	4.6 ± 0.2

remains unclear whether the Cretaceous granitoid magmatism was generated in one or two stages.

In this paper, the manifestations of this magmatism are not considered in detail, and the available data are reported for comparison. A representative sample (Table 2, no. 424-2) characterizes one of the granitoid massifs in the upper reaches of the Pravaya Kolpakova River (Fig. 1). According to the description of M.V. Luchitskaya, this biotite gneissic granite has a hypidiomorphic, locally, poikilitic texture and consists of variable proportions of quartz, plagioclase, K-feldspar, and biotite. This sample defined an age of 80.2 ± 0.9 Ma [17].

The Eocene granitoid massifs occur in various areas of the Kamchatka region (Fig. 1). In the Malka Uplift of the Sredinny Range, this age group includes [17] equigranular granites of the Poperechnaya, Krutogorova, Pravaya Kolpakova, and other rivers. According to Luchitskaya et al., the equigranular granites cut across the metamorphic rocks of the Kolpakova Group, the Krutogorovskie granites, the "autochthonous" complexes of the Kheivan Formation, and the thrust zone and "allochthon" of the Andrianovskaya Formation [17]. Eocene granitoids have not been identified during the geological survey within the Sredinny Range. At the same time, the rocks of the late phase of the Late Cetaceous Kol'skii Complex define U–Pb zircon ages within 48–49 Ma [8]. Samples of equigranular granites (Table 2, nos. 416/1, 437/4, and 439/1) were taken from the massifs that intrude the metamorphic schists and gneisses of the Kamchatka Group. M.V. Luchitskaya described them as muscovite or two-mica granites, which, in addition to quartz, plagioclase, and K-feldspar, contain garnet, apatite, zircon, and titanite. The granites are characterized by their hypidiomorphic texture. According to [17], the U–Pb SHIMP zircon data indicate the Early Eocene (about 52 Ma) age of these granitoids.

One of the largest Eocene intrusive massifs, the Shipunsky Massif, is located at the Shipunsky Cape in southeastern Kamchatka (Fig. 1). The massif's age was earlier considered as Oligocene on the basis of its localization within the Eocene Kubovskaya Formation and the presence of gabbroid and quartz diorite pebbles in the conglomerates of the Late Oligocene–Late Miocene Tyushevskaya Formation [8]. The obtained isotope datings (Table 1) significantly specify its formation age.

The massif is 130 km^2 in area and, according to the geophysical data, is considered as a laccolith-like body [16]. It consists of two phases. The rocks of the first phase are made up of hornblende–pyroxene; two-pyroxene; two-pyroxene–olivine gabbros and gabbronorites; and, more rarely, leucogabbros. The second phase is represented by hornblende and biotite–amphibole quartz diorites, granodiorites, and plagiogranites. In the upper reaches of the Belaya River, the intrusive bodies are situated among the siliceous–terrigenous rocks, which presumably should be ascribed to the Paleocene–Eocene Veaitymlyvayam Sequence (Fig. 1). They are represented by small crosscutting bodies of amphibole and biotite–hornblende granites and granodiorites. The age of one of these bodies was

Table 2. Representative analyses of the intrusive rocks of Kamchatka

Complex	Creta-ceous	Early Eocene			Eocene					
Massif	Pravaya Kolpak-ova R.	Poperechnaya R.			Belaya R.			Shipunsky		
Sample no.	424/2	416/1	437/4	439/1	1778/1	1783	1786	1014	1053	1096
Ordinal no.	1	2	3	4	5	6	7	8	9	10
SiO_2 (%)	67.73	68.62	73.95	74.51	67.04	72.37	73	48.9	49.76	52.51
TiO_2	0.74	0.49	0.02	0.1	0.44	0.34	0.3	0.28	0.81	0.52
Al_2O_3	14.7	15.62	15.32	14.69	16.13	14.52	13.32	20.67	17.68	20.68
Fe_2O_3	5.86	4.34	1.14	2.27	0.94	2.8	0.46	7.56	12.61	6.82
FeO					2.53		1.58			
MnO	0.07	0.06	0.08	0.04	0.12	0.11	n.d.	0.14	0.21	0.11
MgO	1.24	1.31	0.17	0.44	1.28	1.24	0.99	7.14	5.09	6.98
CaO	3.32	2.83	0.35	1.01	5.04	2.01	1.68	13.36	11.12	10.4
Na_2O	3.85	4.07	4.19	4.37	3.8	3.56	3.8	1.64	2.43	1.22
K_2O	2.27	2.48	4.69	2.52	2.08	3.38	3.76	0.28	0.2	0.75
H_2O-					0.5		0.28			
H_2O+					0.61		0.77			
P_2O_5	0.22	0.18	0.09	0.04	0.12	0	0.02	0.02	0.1	
Total	100	100	100	99.99	100.19	99.99	99.7	99.99	100.01	99.99
Rb (ppm)	88.37	110.09	61.69	60.56	71.50	115.15	106.89	3.11	1.92	11.49
Sr	196.33	271.07	35.33	160.95	243.74	175.56	172.35	255.62	355.36	412.50
Y	44.58	12.34	20.71	27.18	22.74	25.42	25.78	5.53	9.66	9.93
Zr	280.65	156.37	39.39	73.90	165.11	165.39	194.11	6.84	11.43	22.52
Nb	8.86	4.67	0.14	3.83	7.06	7.27	6.86	3.36	0.88	0.65
Cs	3.93	4.96	1.86	1.17	2.50	2.60	1.54	0.00	0.02	0.37
Ba	675.11	844.66	281.44	658.81	359.93	660.26	663.57	53.79	85.70	173.66
La	35.37	17.78	3.54	15.76	22.34	20.73	33.82	0.90	1.28	3.81
Ce	79.64	37.90	7.66	35.81	45.79	45.61	71.77	2.44	3.49	9.68
Pr	9.62	4.35	0.86	4.19	5.16	5.06	7.94	0.40	0.60	1.41
Nd	38.33	16.50	3.06	15.75	19.42	19.09	27.64	1.98	3.32	6.54
Sm	8.76	3.61	0.89	3.84	4.01	4.10	5.06	0.62	1.16	1.77
Eu	1.33	0.88	0.07	0.39	0.76	0.58	0.34	0.42	0.66	0.44
Gd	8.28	2.95	1.51	4.09	3.62	3.88	4.08	0.83	1.53	1.92
Tb	1.30	0.42	0.39	0.71	0.56	0.62	0.64	0.14	0.26	0.31
Dy	7.46	2.15	2.81	4.19	3.38	3.83	3.96	0.95	1.84	1.95
Ho	1.50	0.39	0.59	0.83	0.70	0.81	0.84	0.22	0.41	0.40
Er	3.96	1.03	1.70	2.21	2.00	2.35	2.46	0.62	1.15	1.10
Tm	0.56	0.14	0.27	0.31	0.31	0.36	0.39	0.09	0.18	0.16
Yb	3.52	0.89	1.85	1.88	2.01	2.40	2.55	0.64	1.14	1.07
Lu	0.52	0.13	0.25	0.27	0.31	0.37	0.39	0.09	0.18	0.16
Hf	7.27	4.09	1.98	2.69	4.13	4.39	5.30	0.18	0.42	0.59
Ta	0.49	0.38	0.01	0.16	0.64	0.64	0.78	0.10	0.02	0.05
Th	11.68	6.10	0.43	5.01	8.09	9.85	11.73	0.11	0.09	0.15
U	2.55	1.70	0.57	1.21	2.97	2.36	1.86	0.02	0.05	0.16

Table 2. (Contd.)

Complex	Eocene						Miocene–Pliocene			
Massif	Shipunsky				Shamanka R.		Kensol R.			Akhomten
Sample no.	1074	1023	1002	1026	1651	1654	3735	3704	2003/2	8589
Ordinal no.	11	12	13	14	15	16	17	18	19	20
SiO_2 (%)	52.84	53.4	64.27	68.92	63.14	68.13	60.72	66.14	67.74	46.85
TiO_2	0.9	0.77	0.58	0.35	0.62	0.39	0.89	0.76	0.41	0.83
Al_2O_3	16.74	17.87	15.86	15.42	16.07	15.46	15.51	15.48	15.15	20.11
Fe_2O_3	11.19	9.75	6.44	4.13	6.42	5.18	4.6	2.55	5.21	13.11
FeO							3.45	1.72		
MnO	0.22	0.15	0.09	0.06	0.1	0.1	0.16	0.11	0.08	0.2
MgO	4.64	5.06	2.49	1.5	3.36	1.36	2.68	1.85	1.42	5.88
CaO	9.48	9.12	5.13	4.09	4.37	3.88	5.7	4.44	3.65	10.72
Na_2O	3.02	3.13	3.49	3.61	3.5	3.3	3.6	4.09	3.61	2.05
K_2O	0.76	0.64	1.54	1.84	2.3	2.18	1.92	2.61	2.6	0.23
H_2O-							0.08	0.11		99.98
H_2O+							0.6	0.23		
P_2O_5	0.22	0.1	0.11	0.1	0.131	0.07	n.d.	n.d.	0.05	0.02
Total	100.01	99.99	100.00	100.02	100.01	100.05	99.91	100.1	99.92	100
Rb (ppm)	8.19	8.73	21.04	25.31	76.93	69.07	57.15	59.94	61.47	4.19
Sr	317.36	429.03	410.47	380.11	403.50	431.30	545.45	482.67	422.88	460.68
Y	17.04	16.36	22.06	9.95	19.48	15.60	19.80	14.73	13.66	
Zr	48.24	34.13	143.41	136.56	202.32	158.44	87.57	95.85	143.49	14.48
Nb	0.23	4.85	2.10	1.21	7.35	5.88	4.05	4.02	4.61	0.07
Cs	0.28	0.13	0.13	0.25	3.34	2.74	1.45	1.26	1.80	0.62
Ba	191.60	144.36	394.93	374.16	554.74	525.00	1072.79	915.33	862.72	106.28
La	3.79	5.90	9.12	8.28	19.89	17.27	10.25	15.82	11.73	1.40
Ce	10.32	16.01	23.76	17.91	42.10	35.53	23.04	32.63	24.65	3.47
Pr	1.70	2.45	3.42	2.27	5.01	3.99	3.06	3.75	2.96	0.51
Nd	8.61	11.79	15.48	8.97	19.54	15.37	13.49	14.16	11.29	2.58
Sm	2.58	3.20	3.73	1.84	4.07	3.07	3.22	2.75	2.35	0.82
Eu	0.95	0.97	0.92	0.61	1.12	1.03	1.07	0.80	0.70	0.45
Gd	2.97	3.28	3.57	1.71	3.71	2.76	3.05	2.34	2.13	0.99
Tb	0.49	0.50	0.56	0.24	0.54	0.39	0.47	0.35	0.31	0.17
Dy	3.26	3.23	3.28	1.50	3.13	2.36	2.91	2.12	1.94	1.19
Ho	0.71	0.66	0.70	0.32	0.64	0.47	0.61	0.45	0.40	0.26
Er	2.04	1.85	1.99	0.89	1.78	1.29	1.76	1.25	1.21	0.77
Tm	0.31	0.26	0.31	0.13	0.26	0.19	0.27	0.20	0.20	0.12
Yb	2.00	1.63	1.96	0.94	1.72	1.31	1.75	1.30	1.40	0.80
Lu	0.30	0.24	0.31	0.16	0.28	0.20	0.26	0.21	0.23	0.12
Hf	1.25	0.94	3.81	3.79	5.33	3.77	2.27	2.46	3.93	0.41
Ta	0.01	0.10	0.58	0.07	0.71	0.42	0.20	0.28	0.38	0.01
Th	0.18	0.40	1.35	4.13	7.00	6.00	2.10	2.81	3.23	0.08
U	0.20	0.29	0.78	1.91	1.31	2.36	0.83	1.18	1.70	0.09

Table 2. (Contd.)

Complex	Miocene–Pliocene								
Massif	Akhomten	Barabsky				Lake Angre	Avachinsky		
Sample no.	8655/1	k-53	k-116	K-47	K-61	k-11	6231	6225/4	6226
Ordinal no.	21	22	23	24	25	26	27	28	29
SiO_2 (%)	61.2	53	55.25	60.98	63.7	58.99	59.88	64.7	64.76
TiO_2	0.7	0.81	0.72	0.75	0.57	0.72	0.69	0.65	0.74
Al_2O_3	17.02	16.96	18.06	16.8	15.51	16.94	16.68	13.79	14.98
Fe_2O_3	2.88	9.79	8.57	2.44	3.31	7.87	1.35	1.34	1.67
FeO	2.29			3.62	2.64		4.31	3.29	2.91
MnO	0.13	0.16	0.13	0.11	0.12	0.12	0.19	0.18	0.09
MgO	1.56	6.24	4.41	3.28	2.26	3.34	2.62	1.93	1.89
CaO	5.43	8.53	7.63	5.31	5.11	6.16	5.15	3.96	4.27
Na_2O	4.11	3.33	3.64	3.38	3.24	3.33	4.46	4.2	4.11
K_2O	2.24	1.01	1.3	2.58	2.4	2.4	2.53	3.11	2.98
H_2O-	n.d.			0.3	0.14		0.03	0.13	0.01
H_2O+	1.7			0.5	0.5		0.9	1.61	0.81
CO_2	n.d.			n.d.	n.d.		0.39	0.36	n.d.
P_2O_5	0.23	0.17	0.21	0.14	0.19	0.15	n.d.	0.18	0.26
Total	99.45	100	99.92	100.19	99.69	100.02	99.43	99.43	99.48
Rb (ppm)	11.05	17.86	28.85	59.02	88.62	57.67	44.69	60.17	50.43
Sr	601.28	556.06	588.00	459.80	343.37	479.44	489.29	366.85	613.17
Y	21.69	16.02	18.11	25.19	22.55	17.56	10.19	26.76	26.44
Zr	65.52	90.31	117.72	160.50	172.30	195.44	56.54	231.82	123.94
Nb	1.62	1.98	18.37	4.45	4.95	4.59	6.94	7.93	8.07
Cs	0.39	1.61	1.06	1.12	2.12	1.26	1.10	0.75	1.32
Ba	512.64	371.32	380.61	679.97	803.06	669.97	497.61	621.09	679.74
La	10.17	9.70	12.27	16.27	16.97	11.49	12.27	15.20	16.29
Ce	23.64	22.88	29.01	37.43	37.86	27.90	24.06	35.25	37.89
Pr	3.32	3.14	3.84	4.85	4.57	3.83	2.77	4.66	5.06
Nd	15.25	13.88	16.40	20.36	17.99	16.16	10.53	19.51	21.99
Sm	3.73	3.31	3.68	4.54	3.80	3.58	2.03	4.54	5.17
Eu	1.16	1.04	1.11	1.04	0.78	0.88	0.90	0.93	1.40
Gd	3.65	3.23	3.43	4.18	3.56	3.28	1.76	4.25	4.85
Tb	0.56	0.48	0.52	0.64	0.55	0.49	0.26	0.67	0.75
Dy	3.37	2.96	3.25	3.91	3.33	3.05	1.55	4.03	4.38
Ho	0.71	0.62	0.68	0.80	0.71	0.66	0.31	0.86	0.89
Er	2.01	1.73	1.91	2.27	2.07	1.87	0.87	2.46	2.43
Tm	0.29	0.26	0.29	0.35	0.32	0.29	0.13	0.38	0.36
Yb	1.85	1.69	1.87	2.26	2.16	1.95	0.89	2.47	2.25
Lu	0.28	0.25	0.28	0.35	0.34	0.29	0.13	0.39	0.33
Hf	1.69	2.16	2.80	4.30	4.91	4.74	1.45	6.27	3.16
Ta	0.02	0.15	0.38	0.26	0.43	0.36	0.41	0.54	0.46
Th	2.09	1.67	2.27	3.37	7.91	3.67	1.89	4.50	2.50
U	0.69	0.63	0.86	1.11	2.65	1.67	0.39	1.43	0.83

Table 2. (Contd.)

Complex	Miocene–Pliocene		
Massif	Syrytsin R.	Timonovskaya R.	Ganalsky
Sample no.	3237-66	3189	8131/2
Ordinal no.	30	31	32
SiO_2 (%)	63.65	70.26	60.76
TiO_2	0.57	0.4	0.83
Al_2O_3	15.97	14.96	16.02
Fe_2O_3	6.27	1.05	2.69
FeO		1.47	3.73
MnO	0.1	0.06	0.04
MgO	3.31	0.39	2.47
CaO	3.25	1.8	4.88
Na_2O	4.19	3.74	4.16
K_2O	2.54	4.34	2.88
H_2O-		0.34	
H_2O+		0.95	0.61
P_2O_5	0.15	0.13	0.28
Total	100.03	99.89	99.35
Rb (ppm)	58.72	102.25	63.40
Sr	396.79	252.98	526.70
Y	12.19	14.73	23.09
Zr	127.07	145.46	274.63
Nb	2.89	6.55	8.06
Cs	2.99	1.17	0.95
Ba	481.96	597.05	613.25
La	10.64	16.86	13.28
Ce	24.01	35.74	30.49
Pr	3.04	4.06	4.02
Nd	12.62	14.66	16.83
Sm	2.81	2.81	3.93
Eu	0.66	0.54	0.96
Gd	2.46	2.41	3.69
Tb	0.37	0.37	0.59
Dy	2.22	2.19	3.61
Ho	0.47	0.46	0.74
Er	1.33	1.37	2.18
Tm	0.20	0.22	0.33
Yb	1.31	1.54	2.23
Lu	0.20	0.24	0.34
Hf	3.08	4.38	6.78
Ta	0.26	0.60	0.50
Th	3.26	7.29	2.25
U	1.33	2.63	1.00

determined by the K–Ar method as 36.3 ± 0.8 Ma (Table 1).

The large massif in the upper reaches of the Shamanka River is also ascribed to the Eocene stage (Fig. 1). It cuts across the isoclinally folded terrigenous sequences of the Upper Cretaceous Lesnovskaya Formation and the siliceous–volcanogenic rocks of the Irunei Formation of the same age, as well as the zone of the so-called "Lesnovskii overthrust" [26]. Morphologically, the body is laccolith. The central part of the massif is made up of medium- to coarse-grained amphibole–biotite granites, which outward are gradually replaced by granodiorites and amphibole diorites and sometimes with clinopyroxene and biotite. Wide hornfels zones are developed at the contact with the host rocks. The following ages were determined for the massif by different methods [21]: 45.3 ± 1 Ma (U–Pb method), 44.4 ± 0.1 Ma (Rb/Sr method), 47 ± 1.3 Ma (K–Ar method on biotite), 44 ± 2.5 Ma (K–Ar method on hornblende).

The Miocene–Pliocene intrusive rocks. The magmatic bodies of this age are most widely distributed in Kamchatka and southern Koryakia. Small bodies of mainly diorite–granodiorite composition as an almost uninterrupted band extend from the southwestern part of the Koryak highland via Kamchatka southward of the Great Kurile Range and are spatially associated with two Miocene–Pliocene, essentially, andesitic volcanic belts: the central and southeastern ones. These belts are en-echelon arranged within the Avacha–Kitkhoi zone (Fig. 1). The predominance of definite rock varieties within the magmatic complexes is directly correlated with the size of the massif, its emplacement depth, and degree of erosion.

The following massifs are the most known within Central Kamchatka: the Kirganikskii Massif (about 50 km^2 in exposed area) represented by diorites, quartz diorites, and sometimes diorite porphyrites; the Ozernovsky Massif (32 km^2) consisting of granodiortes and granites; the Kasanga Massif represented by granodiorites, granites, diorites, and monzonites; the Ganalsky Tur Massif represented by diorites and gabbrodiorites; the Kensol Massif (18 km^2) consisting of gabbros, diorites, granodiorites, and granites; the Barabsky Massif (15 km^2) represented by diorites, granodiorites, and granites; and the Nachinkinskoe Zerkal'tse Massif (8 km^2 in area) represented by granodiorites and diorite porphyrites. The Akhomten Massif (130 km^2 in area), one of the largest and best studied massifs, is located in Southern Kamchatka (Fig. 1) among the altered volcanogenic-sedimentary rocks of the Miocene Paratun Formation and has an angular almost isometric shape. Its central and most eroded part is made up of granites, which along the periphery are replaced by granodiorites, diorites, and small exposures of marginal gabbroids.

Already the first summary of the available materials made it possible to subdivide the Neogene intrusions

of Kamchatka [7] into two groups: the largest differentiated bodies of the Early Miocene age and the small manifestations of essentially diorite composition ascribed to the Middle and beginning of the late Miocene. Subsequent studies [18, 23] allowed one to unite the considered bodies into Miocene gabbro-granodiorite formations. The massifs were arranged into two types: (1) Early Miocene massifs that were formed during two phases and have no direct links with volcanic manifestations and (2) Late Miocene monophase intrusions representing "volcanic roots." As is seen from Table 1, such an interpretation of the age was mainly confirmed with some younging (for the massifs of the second type) to the lower Pliocene.

The intrusive massif of the Kensol River (about 18 km^2 in area) is the best studied massif and represents a typical example of the two-phase manifestations (Fig. 2). The host rocks are metamorphosed siliceous-silty and volcanic-pyroclastic rocks of the Late Cretaceous Irunei Formation. The localization of the intrusive massif is controlled by a large flexure-like fold. The detailed structural and gravimetry analysis [13, 14] showed that the massif has an asymmetric mushroom shape with a subsequent gentle and steep dip in the western direction. The labradorites, gabbros, and gabbrodiorites of the first phase as individual bodies are localized in the northwestern part of the massif. The rocks of the second phase, which occupies the most part of the massif, are represented by quartz diorites, granodiorites, and granites. They contain through (intratelluric) mineral generations: plagioclase ($An_{51–56}$); amphibole; and possibly clinopyroxene, whose single grains occur in the rocks of the second intrusive phase. These features combine all the rock varieties into a common differentiation series. Noteworthy is the presence of numerous small (from 0.5–1 to 2–3 cm) schlierens, which sometimes contain remains of fine-grained hornfelsed material.

The monophase massifs are typically represented by the series of intrusive massifs and individual intrusions of the Avacha–Kitkhoi tectonic zone (Fig. 1, 3).[1] Their structure was described in detail in works [3, 6, 12]. Four intrusive massifs are located along the arc, the Avacha Range (Fig. 3), and further to the upper reaches of the Kitkhoi and Nalacheva rivers (Fig. 1): the Avachinsky Massif (about 25 km^2, gabbros, gabbrodiorites, diorites, granodiorites, and granites), the Timonovsky Massif (about 10 km^2, gabbros, gabbrodiorites, diorites, and granodiorites), the Syrytsin Massif (about 14 km^2, gabbrodiorites and diorites), and the Kitkhoi Massif (about 30 km, gabbros, gabbrodiorites, and diorites). They are localized within the long-evolving domal-ring structures restricted to the variably uplifted blocks of the considered tectonic zone [3]. The deepest seated Avachinsky Massif is contained in the metamorphosed terrigenous rocks of the Late Cretaceous Khozgon Formation and the volcanogenic pyroclastic rocks of the Miocene Paratun Formation. The shallower Timonovsky, Syrytsin, and Kitkhoi massifs are completely located among the volcanic rocks of the Paratun Formation. These massifs are typically devoid of schlierens, except for single mainly amphibole accumulations or fine-grained melanocratic segregations.

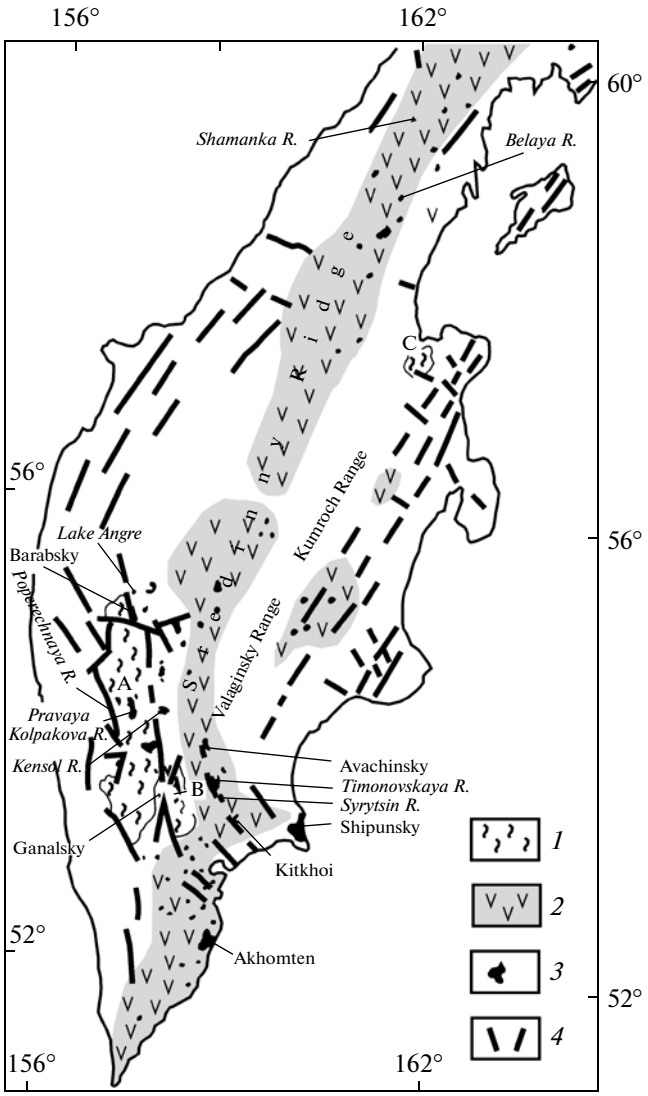

Fig. 1. Distribution scheme of the Late Cretaceous–Pliocene magmatic complexes of Kamchatka.

(*1*) exposures of the rocks of the metamorphic basement: A—Sredinny Massif, (B) Ganalsky Massif, (C) Khavyven Uplift; (*2*) manifestations of the Neogene volcanism; (*3*) granitoid massifs and intrusive bodies; (*4*) main faults.

ANALYTICAL METHODS

The rock-forming oxides were determined by conventional "wet" chemistry at the Analytical Center of the Institute of Volcanology and Seismology of the Far

[1] The Kitkhoi Massif is not shown in Fig. 3.

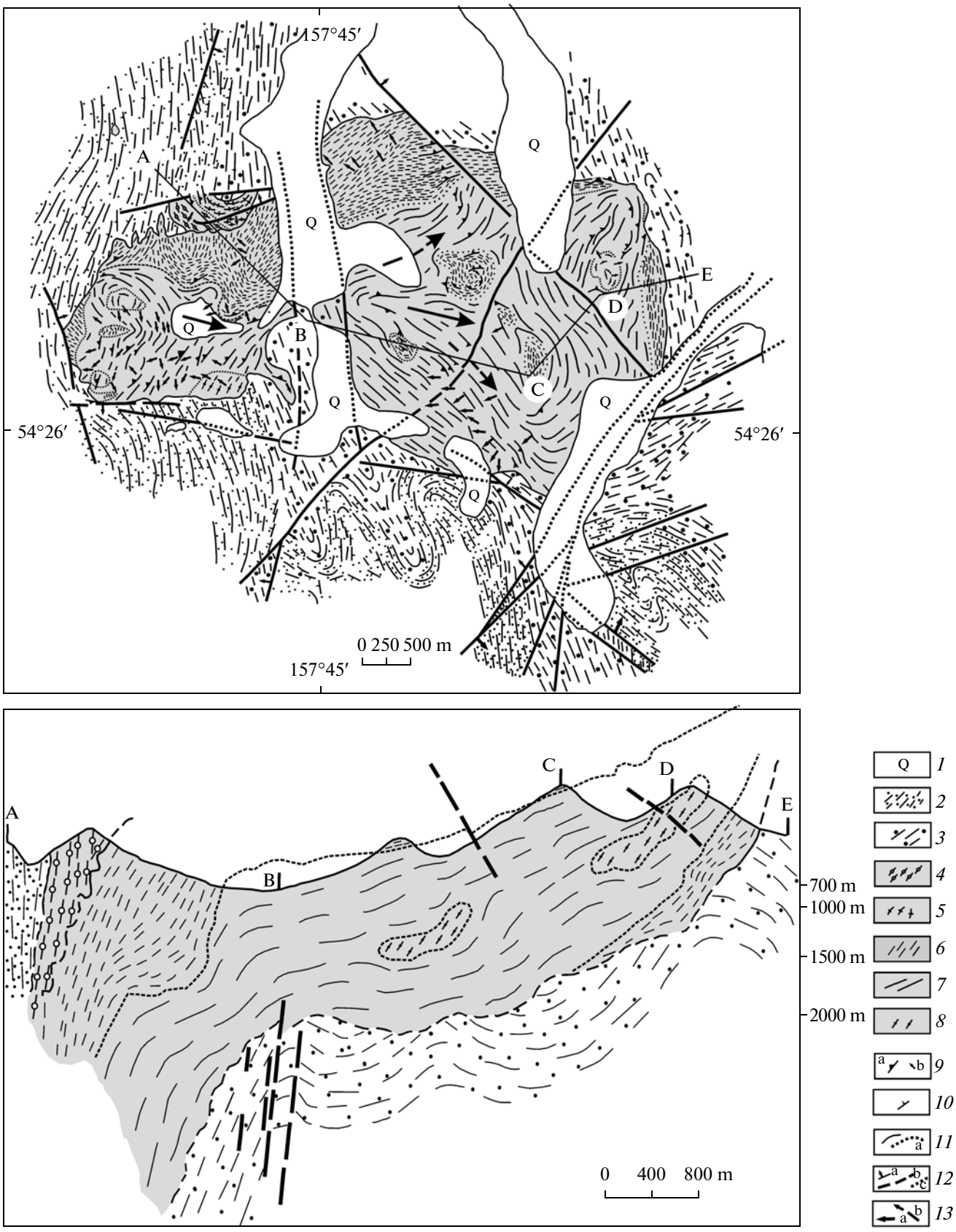
157°45′
54°26′
A
B
C
D
E
Q
0 250 500 m
0 400 800 m
700 m
1000 m
1500 m
2000 m
1
2
3
4
5
6
7
8
9
10
11
12
13

Fig. 2. Geological map and inferred geological section of the Kensol River Massif.

(*1*) Quaternary deposits; (*2*) Siliceous–clayey and sandy–siliceous rocks of the Irunei Group (K_2ir); (*3*) volcanogenic–siliceous rocks of the Irunei Group (K_2ir); (*4*) gabbros; (*5*) gabbrodiorites; (*6*) quartz diorites; (*7*) granodiorites; (*8*) granites; (*9*) orientation of prototectonic elements (a) planar and (b) linear; (*10*) bedding of the host rocks; (*11*) geological boundaries, (a) including petrographic varieties of the rocks; (*12*) tectonic disruptions: (a) traced (the arrow shows a dip of the fault plane), (b) inferred, (c) hidden beneath alluvium; (*13*) direction of movement of the magmatic material during filling of the intrusive chamber: (a) main direction, (b) direction of lateral movement; (ABCDE) line of the geological section. Compiled using the materials of A.V. Koloskov and G.B. Flerov.

East Branch of the Russian Academy of Sciences and by XRF at the Institute of Geology of Ore Deposits, Petrography, Mineralogy, and Geochemistry of the Russian Academy of Sciences in Moscow. The trace elements were determined by ICP-MS with a relative error of 5–10% at the Institute of Analytical Instrument Making of the Russian Academy of Sciences. The Nd and Sr isotope compositions were analyzed at the Geological Institute of the Kola Scientific Center of the Russian Academy of Sciences in Apatity. The method of the Sm–Nd analysis was described in detail in [11, 15]. The Sr isotope composition in all the measured samples was normalized to a value of 0.71034 ± 0.00026 as recommended for NIST SRM-987. The errors in the measurement of the Sr isotope composition (96% confidence level) were no more than 0.04%, and those of the Rb/Sr ratio, 1.5%. The laboratory blank was 2.5 ng for Rb and 1.2 ng for Sr. In order to obtain the rock's age (K–Ar method), the content of radiogenic ^{40}Ar was determined in the 0.5–0.25 fraction on an MI-1201IG mass spectrometer at the Institute of Geology of Ore Deposits, Petrography, Mineralogy, and Geochemistry of the Russian Academy of

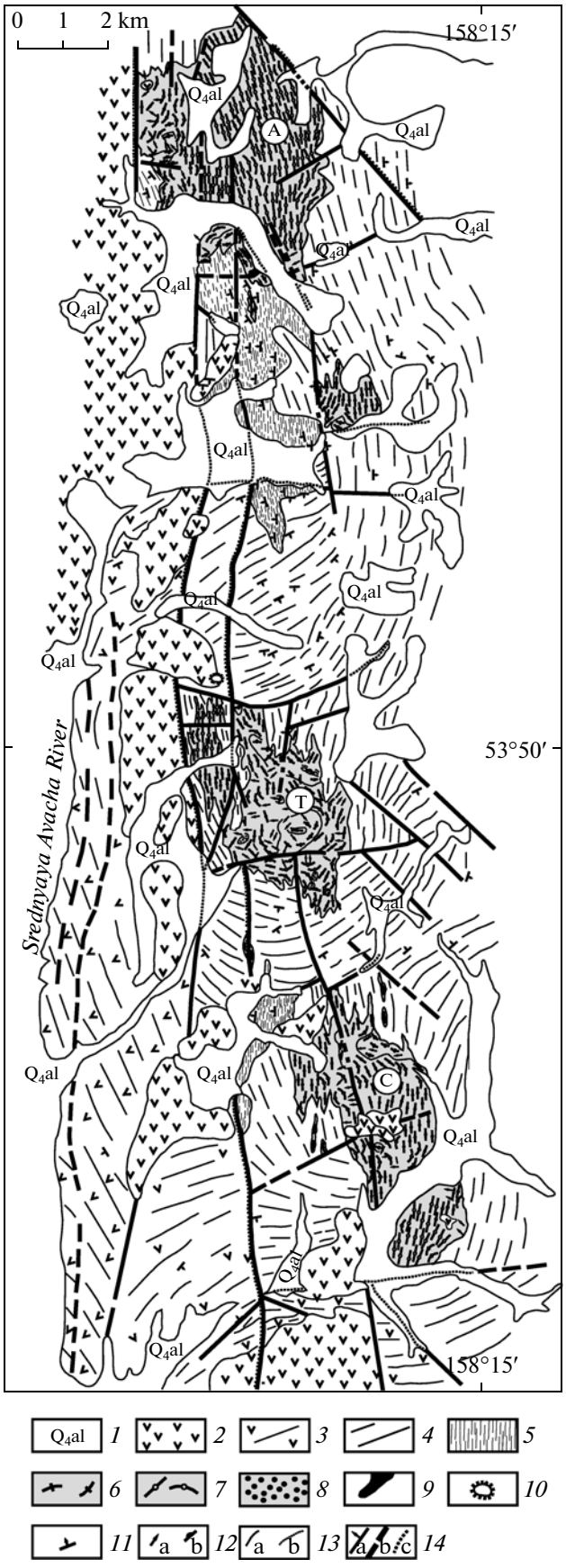

Fig. 3. Geological map of the Avachinsky Range area.

(*1*) alluvial deposits, (*2*) Quaternary andesites, basalts, and the corresponding pyroclastic rocks; (*3*) andesites, basalts, and the corresponding pyroclastic rocks of the Late Miocene–Pliocene Alnei Group (Nal); (*4*) andesites, basalts, and the corresponding pyroclastic rocks of the Miocene Paratun Formation (N_1pr); (*5*) clayey shales, siltstones, and sandstones of the Late Cretaceous Khozgon Formation (K_2hz?); (*6*) porphyritic gabbros and gabbrodiorites; (*7*) diorites; (*8*) granodiorites; (*9*) granites; (*10*) Quaternary scoria cones; (*11*) dip and strike of the bedding; (*12*) prototectonic elements: (a) linear, (b) planar orientation; (*13*) geological boundaries (a), including petrographic rock varieties (b); (*14*) tectonic disruptions: (a) proved, (b) inferred, (c) hidden beneath alluvium (the arrows show the orientation of the fault plane; the dashes are shown from the side of the hanging block). (A) Avachinsky Massif; (T) Timonovskaya intrusion; (C) "Syrytsin" intrusion. Compiled by A.V. Koloskov using the materials of O.B. Selyangin, S.E. Aprelkov, and B.K. Dolmatov.

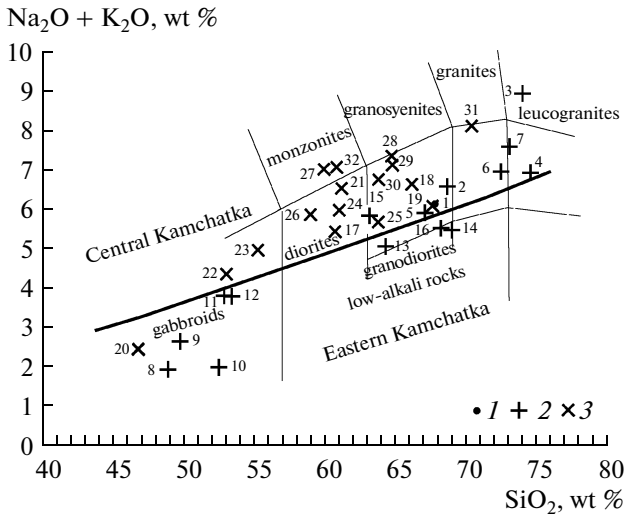

Fig. 4. Diagram of the SiO_2–total alkalinity for the rocks of the intrusive massifs of Kamchatka.
(*1–3*) complexes of intrusive massifs: (*1*) Cretaceous; (*2*) Eocene; (*3*) Miocene–Pliocene. The numbers in the diagrams correspond to the ordinal numbers in Table 2. The boundary lines and compositional fields are shown on the basis of the modified [27] TAS diagram.

Sciences using the isotope dilution method with a ^{38}Ar monoisotope as the tracer. The geochronological calculations were performed using the decay constants recommended by the International Commission on Geochronology [30].

COMPOSITIONAL FEATURES

Petrogenic Elements

As is seen from the presented materials (Table 2, Fig. 4), the considered intrusive manifestations are characterized by a wide range of SiO_2 content (from 47 to 74.5%) at relatively narrow variations of the other major components. The total alkali content depending on the SiO_2 varies from 2 to 9% (Fig. 4). Regardless of age, the main part of the data points is plotted in the field of moderately alkaline compositions. The diorites of the Avachinsky and Ganalsky massifs have the most alkaline composition: their data points plot in the monzonite field. The gabbroids of the Akhomten and Shipunsky massifs, as well as the granodiorites of the latter, are distinguished in a separate group of the least alkaline rocks. In general, this indicates transverse zoning, which began to appear at Kamchatka already in the Eocene time.

With the increasing SiO_2 content, the rocks show a decrease in Al_2O_3, CaO, and MgO. The highest Al_2O_3 contents in some gabbros of the Shipunsky and Akhomten massifs, in combination with the elevated CaO contents, may be related to the plagioclase cumulus enrichment.

Trace Elements

In the primitive mantle-normalized [31] spider diagrams (Fig. 5), the rocks of all the considered intrusive complexes demonstrate a compositional peculiarity typical of the island-arc series: they are enriched in light lithophile elements (LILE) and light rare-earth elements (LREE) relative to the high-field strength elements (HFSE) and middle (MREE) and heavy (HREE) rare-earth elements. All the diagrams display well pronounced Nb, Ta, Ti, and Eu negative anomalies (except for Eu in the Shipunsky and Akhomten massifs). A positive Sr anomaly typical of the island-arc series is observed practically in all the samples of the Miocene–Pliocene complex and in the gabbroids of the Shipunsky Massif, and it is practically absent in the granitoids of the Cretaceous and Eocene complexes. The granodiorites and granites of the Sredinny Range, unlike the same rocks of Eastern Kamchatka, in addition to elevated potassium alkalinity, show enrichment in fluid-mobile components (Rb, Th, and U; Table 2 and Fig. 5) and higher $(La/Yb)_n$ ratios ($(La/Yb)_n$ = 7.2–14 as compared to 4–6 in the same rocks of the Shipunovsky Massif).

Isotope Composition of the Rocks

The isotope composition of the rocks of the studied massifs is reported in Tables 3 and 4. It is seen that the rocks differ in their Nd and Sr isotope composition: $\varepsilon_{Nd}(T)$ varies from –0.36 to +9.3, while $I_{Sr}(T)$ varies from 0.70350 to 0.704843. In terms of isotope variations, the rocks of the massifs are subdivided into three groups: I—Cretaceous and Eocene massifs of Central Kamchatka with a narrow range of variations: $\varepsilon_{Nd}(T)$ = 0–3.3 and $I_{Sr}(T)$ = 0.7043–0.7048; II—Eocene granitoids of the Shipunsky Massif with extremely elevated values of $\varepsilon_{Nd}(T)$ = 9.2–9.3 and lowered values of $I_{Sr}(T)$ = 0.7036; and III—Miocene–Pliocene complexes with wide variations: $\varepsilon_{Nd}(T)$ = +3.42 to +8.6 and $I_{Sr}(T)$ = 0.7035–0.7044.

DISCUSSION

There are numerous geochemical classification diagrams that take into account the composition of the granitic rocks and the differences in their tectonic setting [29]. However, their critical analysis showed that they are not always reliable [28]. The rocks of the same composition and structural position can plot in different fields, or rocks formed in different geodynamic settings can be juxtaposed in one field. For instance, the data points of the rocks of all the studied massifs in the Rb–(Nb + Y) diagram [29] fall in the volcanic-arc field (Fig. 6). At the same time, according to [17], the data points of the Late Cretaceous–Eocene granites fall in the collisional field in the diagram proposed by Velikoslavinskii [2] for the geodynamic discrimination of granitoids. It is likely that the geochemical characteristics of the granitoids primarily reflect the compo-

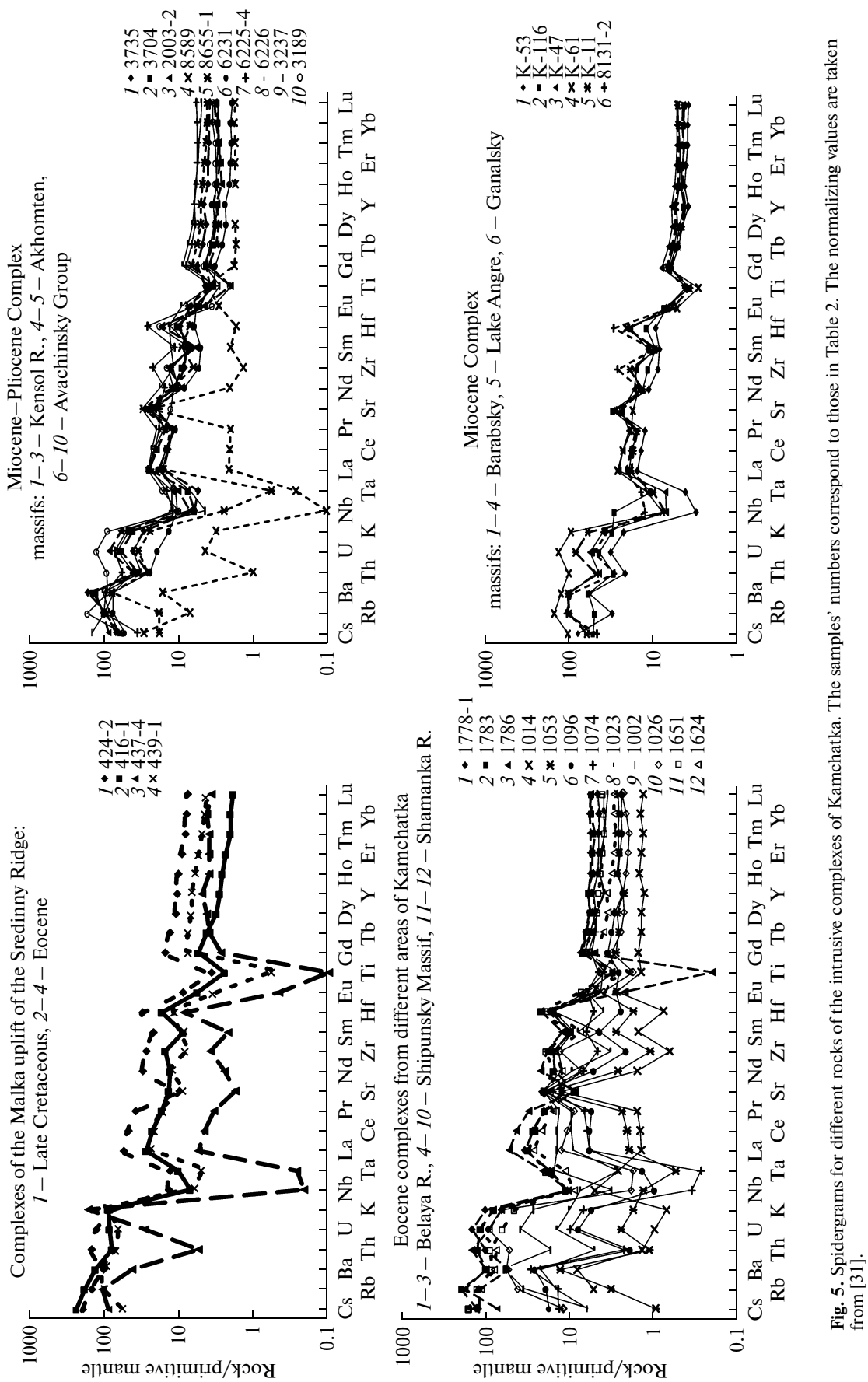

Fig. 5. Spidergrams for different rocks of the intrusive complexes of Kamchatka. The samples' numbers correspond to those in Table 2. The normalizing values are taken from [31].

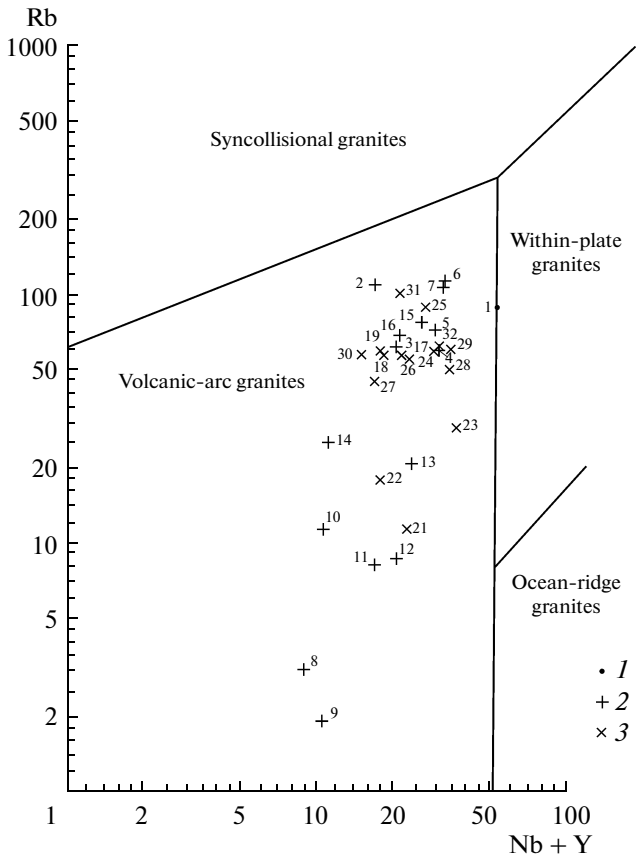

Fig. 6. Rb–(Nb + Y) discriminant diagram for granitoids having different structural positions. The symbols are shown in Fig. 4.

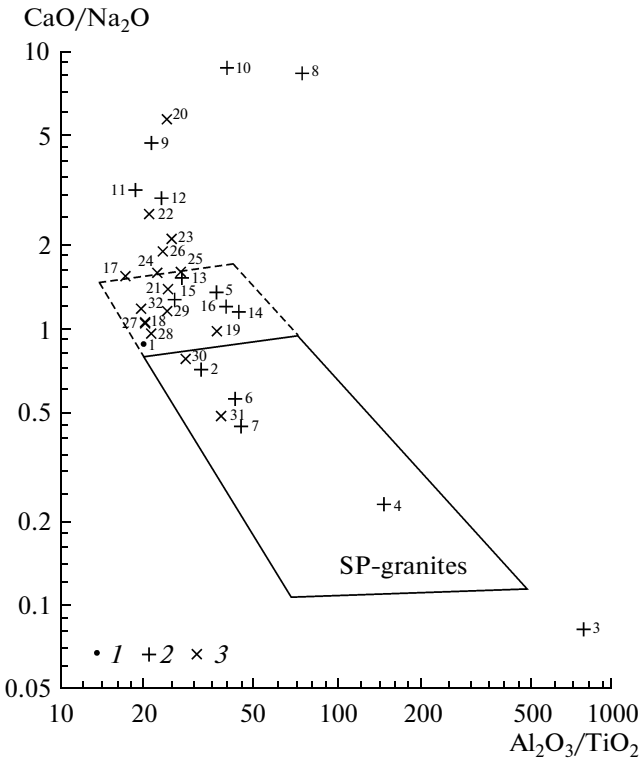

Fig. 7. CaO/Na_2O–Al_2O_3/TiO_2 diagram for the rocks of different intrusive complexes of Kamchatka.
The symbols are shown in Fig. 4.

sition of the parental melts and the crystallization conditions, whereas the role of the tectonic setting is of subordinate significance. Therefore, the main attention further will be focused on the composition of the initial melts and their sources for the considered intrusive complexes and their further evolution.

Petrological–Geochemical Types of Intrusive Rocks and the Source's Composition

An SP-diagram in the coordinates CaO/Na_2O–Al_2O_3/TiO_2 was proposed by Sylvester [32] to characterize high-aluminous (peraluminous, plumasite) granites (Fig. 7), which were supposedly formed via melting of metasedimentary protolith. The data points of the Cretaceous, as well as the Eocene, massifs of Central Kamchatka are completely plotted in this field or close to its boundaries (possibly, they should be wider). Their position indicates that that the massifs of this age are ascribed to the same SP type of granitoids or to some intermediate group, which was presumably also contributed by a metasedimentary protolith. The compositions of the rocks of the Shipunsky Massif fall far from this field and only the extreme most felsic varieties are plotted in some "intermediate" field. This massif can be ascribed to the I-type (igneous rocks and, judging from the composition, tholeiitic series), which was formed by crystallization differentiation of primary basaltic melts. The data points of the Miocene–Pliocene granitoids are plotted either in the field of the "intermediate group" or far from the field of SP granites. However, several data points of the Timonovsky Massif also plot in this field. Their formation was presumably controlled by both the melting of metasedimentary rocks and the crystallization differentiation.

In the diagram showing the relations of the large ion lithophile elements (Fig. 8) that is used for the identification of the metasources [32], the data points of the granitoids of the Sredinny Range are plotted in the melting trend of psammitic material. The composition of the Shamanka granitoids can be derived by the melting of the pelitic source, while the felsic rocks of the Belaya River are clustered separately: the data point of the granodiorite (no. 5) falls in the trend of metapelite melting, while the granites (nos. 6–7) "require" a psammitic source for their formation. It is noteworthy that the data point of the granodiorite from the Belay River (no. 5) lies in the proximity of the compositions (after [17]) of the metasedimentary rocks of the Kolpakova Group and the schists of the Kamchatka Group. This fact may indicate the wider distribution of metamorphic rocks similar to those

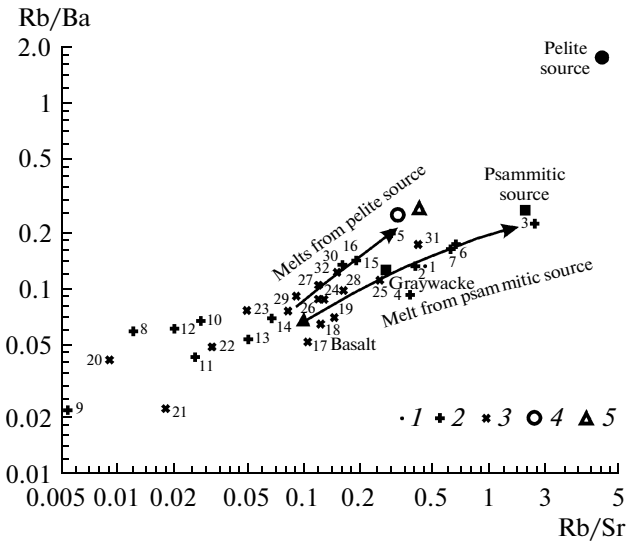

Fig. 8. Rb/Ba–Rb/Sr diagram for the rocks from different intrusive complexes of Kamchatka.

(*1–3*) the same as in Fig. 4: (*4*) schists of the Kamchatka Group; (*5*) metasedimentary rocks of the Kolpakova Group (4—5) after [17]: the distinguished symbols are the calculated compositions of the sources after [17]. The numbers in the plot correspond to the ordinal numbers in Table 2.

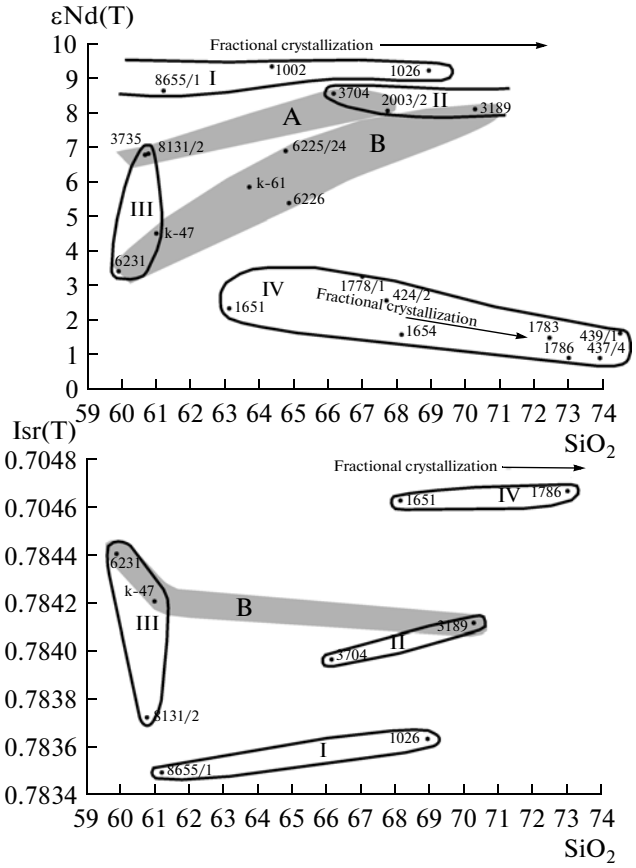

Fig. 9. Variations of $\varepsilon_{Nd}(T)$ and $I_{Sr}(T)$ versus SiO_2 in the rocks of different intrusive complexes of Kamchatka.

The sample numbers correspond to those presented in Table 2. (A–B) fields of the melt mixing for the rocks of the Kensol River and Ganalsky massifs (A) and the Avachinsky (B) groups. The Roman numerals show the compositions of the different sources.

exposed in the Malka Uplift of the Sredinny Range of Kamchatka. This suggestion is consistent with the considerations of Aprelkov and Popruzhenko [1], who distinguished the common Ukelayat–Sredinny Block. According to [1], this structure "occupies a significant part of the Koryak highland and, as narrow band, is traced up to the Sredinny Kamchatka Massif." It is considered that this block has a continental nature and represents either a detached [1] or advanced [20] fragment of the Omolon Massif. The position of the data points of the Pliocene Barabsky and Timonovsky massifs is unclear. The first is not ascribed to the SP type, while the second will be considered below in discussing the isotope characteristics.

Though we have no isotope data on the gabbroids of the Shipunsky Massif and the two-phase Miocene massifs, the position of the trends in the diagrams (Figs. 9, 10) suggests that the evolution of their melts was controlled by the interaction of different sources. The first source is characterized by the highest $\varepsilon_{Nd}(T)$ from +8.6 to +11.6 and, correspondingly, the lowest $I_{Sr}(T)$ ($I_{Sr}(T)$ = 0.7030–0.7036). This source is not deciphered in the composition of the granitoids of the Sredinny Range. Its traces are observable in the isotope characteristics of the granodiorites and granites of the Shipunsky Massif (Tables 3, 4); the gabbronorites (ε_{Nd} = + 9.7; $^{87}Sr/^{86}S$ = 0.7030) of the Eocene [8] Yurchik Massif in the Ganalsky Range [33]; and the gabbroids (ε_{Nd} = + 11.6; $^{87}Sr/^{86}Sr$ = 0.70307–0.70345, after [5]), diorites (Sample 8655/1), and granodiorites (ε_{Nd} = + 9.2; $^{87}Sr/^{86}Sr$ = 0.70352, after [5]) of the Akhomten Massif. Close isotope characteristics (ε_{Nd} from +8.9 to +10.4; $^{87}Sr/^{86}Sr$ = 0.7031–0.7035, after [4, 24]) were also found in the most depleted compositions of the amphibolites and the crystalline schists of the Ganalsky metamorphic complex. It could have been formed by the deep differentiation of the parental mantle or the melting of the crystalline protolith, which is similar in composition to the rocks of the Ganalsky Range. Many researchers consider the similar isotope characteristics of the Late Cretaceous–Paleogene [11, 15, 22] or Early Miocene [5] volcanic rocks of Kamchatka as derivations from depleted mantle sources.

The second source also has high values of the Nd isotope composition $\varepsilon_{Nd}(T)$ from +5.7 to +8.5, but it reveals a highly radiogenic strontium isotope composition $I_{Sr}(T)$ = 0.7040–0.7046. This source is not revealed in the composition of the granitoids of the Sredinny Ridge but was unraveled in the isotope characteristics of the granodiorites (Tables 3, 4; sample 3704) and granites (Tables 3, 4 (sample 3189) and

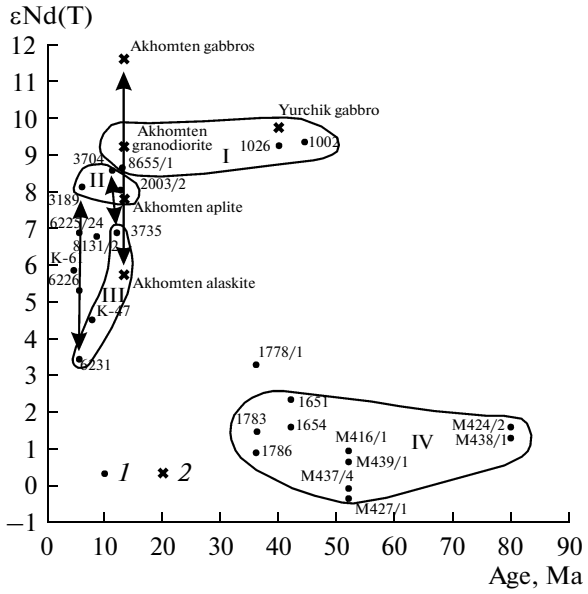

Fig. 10. $\varepsilon_{Nd}(T)$ versus age (Ma) for the rocks of different intrusive complexes of Kamchatka.

(*1*) author's data; (*2*) data from [5, 33]. The arrows show the mixing fields of the melts for the rocks of the corresponding massifs. The other symbols are shown in Fig. 9.

Table 3 (sample 2003/2)) of the Miocene massif of the Kensol River and the Pliocene Timonovsky Massif. Traces of this source were discovered in the alaskites ($\varepsilon_{Nd} = +5.7$; $^{87}Sr/^{86}Sr = 0.70462$) and aplites ($\varepsilon_{Nd} = +7.8$; $^{87}Sr/^{86}Sr = 0.7046$) of the Akhomten Massif [5]. Since close isotope characteristics (ε_{Nd} from +9.2 to +10.4; $^{87}Sr/^{86}Sr = 0.7043–0.7048$, according to [4, 24]) were found in some plagiogneisses of the Ganalsky Range, this source could have been formed due to the contamination of the mantle source by crystalline schists, which are compositionally similar to the metamorphic rocks of this range.

The third source with intermediate isotopic characteristics ($\varepsilon_{Nd}(T)$ from +6. 8 to +3.4; $I_{Sr}(T) = 0.7037–0.7044$) manifested itself in the diorites of the Avachinsky (sample 6231), Ganalsky (sample 8131/2), and Kensol River (sample 3735) massifs. Low Nd ($\varepsilon_{Nd}$from −5.0 to −3.8) and high Sr ($^{87}Sr/^{86}Sr = 0.7046$, on the average) isotope characteristics were determined in the granulites of the Ganalsky Ridge [33]. Therefore, this source could have been formed either due to the contamination of the mantle melts by crystalline rocks that are compositionally similar to those exposed in the range area or due to their selective melting.

The fourth source has the lowest $\varepsilon_{Nd}(T)$ (from −0.1 to +2.3) and the highest $I_{Sr}(T)$ (0.7046–0.7048). It is identified in the Cretaceous and Eocene granodiorite–granite massifs of the Sredinny Massif of Kamchatka. A similarly high radiogenic Sr composition was determined in the metamorphic rocks of the Kolpakova and Ganalsky groups of the Malka uplift [4, 24]. The joint analysis of the diagrams in Figs. 9 and 10 provides the following interpretation of the evolution of the considered rocks. The Cretaceous and Eocene granitoids of the Sredinny Range have similar isotope-geochemical compositions, which, in turn, are close to those of the Kolpakova and Kamchatka groups. They could have been formed by the melting of the metapelitic and metapsammitic material of these groups. Similar conclusions were reached in work [17] for the massifs of the Malka uplift. The compositional diversity of the rocks is related to the crystallization differentiation, while the characteristic negative trends in the $\varepsilon_{Nd}(T)–SiO_2$ diagram (Fig. 9) possibly result from the different contribution of minerals with diverse Nd isotope ratios. The gabbroids from the most depleted rocks of the Shipunsky massif were not analyzed for the Nd isotope composition. However, by analogy with the Yurchik Massif of the same age, all the rock diversity was provided by the fractional crystallization from a common mantle source (I). Most of the rocks of the Akhomten Massif were presumably derived from the first source; the contribution of the second source is traced only in the alaskites and aplites. To explain this fact, it was assumed [5] that the rocks of this massif were formed due to the fluid reworking of the surrounding rocks with close Sr isotope characteristics. Such a mechanism cannot be excluded in single cases (during the formation of the "marginal" gabbroids); however, it is hardly suitable for the entire belt of the Miocene massifs. The less depleted compositions of the two-phase massif of the Kensol river show both widespread signs of mixing of two sources ("basaltic (III)" and "rhyolitic (II)") and crystallization differentiation, which are well expressed here judging from the presence of the through intratelluric mineral generations. The enriched compositions of the monophase massifs of the Avacha–Kitkhoi group are more abundant in the mixing products of the "basaltic (III)" and "rhyolitic (II) sources, whereas the products of the intrachamber differentiation are less pronounced. The individual and most enriched compositions of granites (Timonovsky Massif) were completely generated from isotope source II, which is considered to be derived by the melting of the metabasites of the Ganalsky Group, as follows from their isotope composition and position in the melting curves (Fig. 8).

Thus, the Cretaceous time was marked by felsic crustal magmatism confined to the high-grade area (the central part of the Sredinny Range), whereas the Eocene magmatism operated simultaneously in two zones: the crustal magmatism within the Sredinny Range and the mantle gabbro–granite magmatism within the Eastern Kamchatka and Ganalsky Range. In the Miocene, essentially mantle magmatism was preserved in the frontal zone (the Akhomten Massif), while the magmatism in the Sredinny Range and the junction zone with the Southeastern volcanic belt pro-

Table 3. Nd isotope composition in the intrusive rocks of Kamchatka

Sample no.	Massifs	Rock	Age (Ma)	Content ppm		Isotope ratios		$T_{Nd}(DM)$ (Ma)	$\varepsilon_{Nd}(0)$	$\varepsilon_{Nd}(T)$
				Sm	Nd	$^{147}Sm/^{144}Nd$	$^{143}Nd/^{144}Nd$			
M438/1*	Malka uplift	granite	80			0.08254	0.512644	590.3660483	0.11704165	1.282724732
M00424/2*	Malka uplift	granite	80	7.473	33.571	0.134565	0.512687 ± 30	895.053614	0.95584	1.590477
M 427/1*	Malka uplift	granite	52			0.10699	0.512589	803.93035	−0.955840184	−0.360656992
M00439/1*	Malka uplift	granite	52	4.480	19.814	0.136669	0.512650 ± 17	992.5406163	0.234083	0.632474
M00437/4*	Malka uplift	granite	52	1.237	4.541	0.164673	0.512623 ± 8	1641.249824	−0.292604	−0.080114
M00416/1*	Malka uplift	granite	52	3.822	19.331	0.119534	0.512660 ± 6	796.0494974	0.429153	0.941276
1778/1	Belaya R.	granodiorite	36	3.623	17.815	0.122923	0.512789 ± 18	609.2116839	0.945548	3.284722
1783	Belaya R.	granite	36.3	3.809	18.706	0.123096	0.512696 ± 25	766.790048	1.131403	1.472436
1786	Belaya R.	granite	36	4.483	25.131	0.107836	0.512663 ± 19	703.8890346	0.487674	0.89593
1002	Shipunsky	granodiorite	44.5	3.453	14.402	0.144936	0.513101 ± 19	111.3025415	9.031714	9.326668
1026	Shipunsky	granodiorite	40	1.724	8.527	0.122231	0.513091 ± 16	100.3765058	8.836645	9.217637
1651	Shamanka	diorite	42	3.733	18.173	0.124162	0.512738 ± 15	704.4487815	1.950694	2.339665
1654	Shamanka	granodiorite	42	2.820	14.137	0.120576	0.512698 ± 19	742.7969959	1.170417	1.578524
6226	Avachinsky	granodiorite	5.5	4.742	20.524	0.139675	0.512907 ± 7	503.8543393	5.247368	5.287454
6225/4	Avachinsky	granodiorite	5.5	4.199	19.092	0.132968	0.512988 ± 12	308.7904238	6.82743	6.872244
6231	Avachinsky	diorite	5.5	1.989	11.828	0.101653	0.512810 ± 24	465.0541885	3.355194	3.421934
8131/2	Ganalsky	diorite	8.6	3.558	15.637	0.137560	0.512982 ± 20	339.4569318	6.710388	6.775422
3189	Timonovskaya	granite	6	2.754	14.534	0.114527	0.513050 ± 22	155.7998498	8.03686	8.099883
K-61	Barabsky	granodiorite	4.6	3.471	16.367	0.128191	0.512936 ± 19	384.4244684	5.813069	5.853341
K-47	Barabsky	diorite	7.7	4.163	18.792	0.133921	0.512866 ± 33	545.9434857	4.447583	4.509341
8655/1	Akhomten	diorite	13	3.107	12.808	0.146642	0.513076 ± 11	171.1740506	8.544041	8.627346
3704	Kensol	granodiorite	11.3	2.490	13.309	0.113094	0.513070 ± 23	123.1800388	8.426999	8.547773
3735	Kensol	diorite	12	2.822	11.979	0.142408	0.512986 ± 21	353.9746903	6.788416	6.871742
2003/2	Kensol	granodiorite	12.6	2.089	10.468	0.120625	0.513044 ± 15	175.8693097	7.919819	8.042365

Note: * data of M.V. Luchitskaya

Table 4. Sr isotope composition of the intrusive rocks of Kamchatka

Sample no.	Massifs	Rock	Age (Ma)	Content ppm		Isotope ratios;		$I_{Sr}(T)$	$E_{Sr}(T)$
				Rb	Sr	$^{87}Rb/^{86}Sr$	$^{87}Sr/^{86}Sr$		
M00427/1*	Malka uplift	granite	52	152.2	235.7	1.86843	0.706303	0.70484319	5.7907892
M00438/1*	Malka uplift	granite	80	83.41	229.1	1.05328	0.705465	0.704268	−1.97
1786	Belaya R.	granite	36	97.26	162.8	1.728896	0.70555 ± 6	0.70467	2.96
1026	Shipunsky	granodiorite	40	24.75	375.4	0.190780	0.70375 ± 6	0.70364	−11.42
1654	Shamanka	granodiorite	42	60.01	470.3	0.369240	0.70485 ± 13	0.70463	2.54
6231	Avachinsky	diorite	5.5	44.91	517.6	0.250966	0.70443 ± 30	0.70441	−1.16
8131/2	Ganalsky	diorite	8.6	54.82	527.4	0.300723	0.70377 ± 7	0.70373	−10.76
3189	Timonovskaya	granite	6	98.16	253.5	1.120951	0.70422 ± 6	0.70412	−5.23
K-47	Barabsky	diorite	7.7	55.61	450.0	0.357658	0.70425 ± 12	0.70421	−3.94
8655/1	Akhomten	diorite	13	10.19	687.5	0.042891	0.70351 ± 10	0.70350	−13.95
3704	Kensol	granodiorite	11.3	52.14	439.5	0.343418	0.70402 ± 5	0.70397	−7.39

Note: * data of M.V. Luchitskaya

duced mantle–crustal granitoid massifs. It is noteworthy that the crustal material significantly contaminated the mantle sources up to the formation of purely crustal melts in some massifs.

Geodynamic Setting of the Intrusive Magmatism

The Cretaceous granodiorite–granite intrusive massifs are usually located within the granite-gneiss domes: the Khangarsky, Kolpakovsky, Luntovsky, and others of the Sredinny Range of Kamchatka. This fact implies their synorogenic (syncollisional) formation during the main stages of the folding and metamorphism. It should never be forgotten that the Late Cretaceous–Early Paleogene stage was marked by the large-scale manifestation of basaltic magmatism over all Kamchatka, whereas large granitoid intrusions were developed only within the metamorphic rocks of the Sredinny Range. This fact is difficult to explain from the viewpoint of accretionary tectonics. Such a large scale and local development of granite formation can be explained by either the presence of structural–compositional heterogeneity over the entire Sredinny Range of Kamchatka [1] (the remains of the older continental crust and its rejuvenation in the Late Cretaceous–Eocene time [8]) or by manifestation of a heat anomaly due to the breaking up of the lower lithosphere and the protrusion of the asthenosphere [17].

The Eocene stage was responsible for the manifestation of contrasting intrusive magmatism: the crustal magmatism in the Sredinny Range and the essentially mantle magmatism at the southeastern margin and in the Ganalsky Range. According to [17], the Late Cretaceous stage of granite magmatism in the central part of the Sredinny Range of Kamchatka was related to the accretionary setting at the Eurasian margin. These authors relate the Early Eocene stage with the collision between the Achaivayam–Valaginskaya island arc and the Kamchatka margin of Eurasia. However, the Early Eocene massifs of the Malka Uplift cut across the nappe-folded structures (both autochthon and allochthon) formed during collisional events [10, 17, 21]. According to [26], the Shamanka River Massif intruded the folded-thrust structures of the Lesnovsk Uplift, while the intrusions of the Belaya River are typical fissure intrusions. Such relations imply the postcollisional origin of these bodies. The Shipunsky gabbro–granite massif, together with the host volcanogenic rocks (basalt–andesite–dacites) of the Eocene Kubovskaya Formation, belongs to the terrane ensemble of the Eastern peninsulas [25] but bears all the features of the intrusive complex of the island-arc volcanoplutonic formation. Hence, its formation cannot be related to the collisional setting inferred for Eastern Kamchatka in the Eocene [9]. Thus, in terms of their geological position, all the Eocene granitoid massifs are postcollisional.

The Miocene–Early Pliocene massifs are spatially associated with the Neogene volcanic belts, which overprint all the older structures of Kamchatka and south Koryakia. The Miocene time produced hypabyssal fissure-type two-phase massifs of complex structure that have no direct relations with the volcanic complexes. The intense block movements in the Late Miocene–Pliocene were responsible for the formation of shallow-subsurface diorite–granodiorite massifs in the domal-ring structures—centers of volcanic activity.

CONCLUSIONS

(1) The geological evolution of the active continental margin of Kamchatka includes three types of granitoid magmatism: the Cretaceous, Eocene, and

Miocene–Pliocene. The independent Eocene stage was recognized for the first time. The largest scale Cretaceous crustal magmatism was localized exclusively among the crystalline basement of the Sredinny Range of Kamchatka in a setting of intense tectonic movements and metamorphism. The lesser in scale but wider spread Eocene magmatism was represented by the emplacement of crustal granitoid melts in the Sredinny Range and mantle initially basaltic melts, which evolved to granite compositions, in the southeastern part of the peninsula and in the Ganalsky Range. This was the time of the rejuvenation of the older crust and the local formation of new continental crust. Small-scale Miocene–Pliocene compositionally variable crustal–mantle magmatism confined to the volcanic belts participated in the formation of the upper crustal horizons on the already formed crystalline basement.

(2) In general, the more alkaline granodiorites and granites of the Sredinny Range of Kamchatka have enriched isotope compositions and elevated concentrations of Rb, Th, U and LREE as compared to their counterparts in the eastern part of the region.

(3) Among the granitoid magmatism of Kamchatka, only the Cretaceous granitoids could be ascribed to synorogenic (syncollisional) bodies formed at the peak of the folding and metamorphism. The Eocene and Neogene manifestations of the granitoids are controlled by the fault tectonics and were formed at the "postcollisional" stage. The localization of the Early Pliocene massifs of the Avacha–Kitkhoi zone in the domal–ring structures possibly reflects the tectonic features of the en-echelon junction of the volcanic belts of the Sredinny Range and southeastern Kamchatka.

ACKNOWLEDGMENTS

I'm grateful to M.V. Luchitskaya for materials provided, as well as to D.V. Kovalenko for help in obtaining analytical data and the constructive discussion of the manuscript.

REFERENCES

1. S. E. Aprelkov and S. V. Popruzhenko, "The Penzhina–West Kamchatka Folded Zone and the Ukelayat–Sredinny Block in the Structure of the Koryak Highland and Kamchatka," Tikhookean. Geol. **28** (4), 90–104 (2009) [Russ. J. Pac. Geol. **3**, 388–400 (2009)].
2. S. D. Velikoslavskii, "Geochemical Classification of Silicic Igneous Rocks of Major Geodynamic Environments," Petrologiya **11** (4), 363–380 (2003) [Petrology **11**, 327–342 (2003)].
3. *Relationship of Different-Depth Magmatism*, Ed. by K. N. Rudich (Nauka, Moscow, 1982), pp. 61–94 [in Russian].
4. V. I. Vinogradov, M. I. Bujakaite, G. L. Goroshchenko, et al., "Isotopic and Geochronological Features of High-Grade Rocks of the Ganal Massif in Kamchatka," Dokl. Akad. Nauk SSSR **318** (4), 930–936 (1991).
5. V. I. Vinogradov, V. S. Sheimovich, I. I. Vishnevskaya, et al., "The Akhomten Granitoid Massif: A Model Example of Granitization in the Continent–Ocean Transition Zone," Izv. Vyssh. Uchebn. Zaved., Geol. Razved., No. 5, 50–63 (1993).
6. O. N. Volynets and A. V. Koloskov, *Plagioclases from the Quaternary Volcanic Rocks and Shallow Intrusions of Kamchatka* (Nauka, Novosibirsk, 1976) [in Russian].
7. *Geology of USSR. Vol. 31. Kamchatka, Kuril, and Commander Islands* (Nedra, Moscow, 1964), Part 1 [in Russian].
8. *State Geological Map of Russian Federation. 1:1000000. Sheet N-57. Petropavlovsk-Kamchatskii: Explanatory Notes*, Ed. by A. F. Litvinov and B. A. Markovsky (Izd-vo VSEGEI, St. Petersburg, 2006) [in Russian].
9. V. P. Zinkevich, E. A. Konstantinovskaya, N. V. Tsukanov, et al., *Accretionary Tectonics of Eastern Kamchatka* (Nauka, Moscow, 1993) [in Russian].
10. D. V. Kovalenko, *Paleomagnetism of Geological Complexes of Kamchatka and Southern Koryakia: Tectonic and Geophysical Interpretation* (Nauch. Mir, Moscow, 2003) [in Russian].
11. D. V. Kovalenko, V. A. Koloskov, N. V. Tsukanov, and P. I. Fedorov, "Geodynamic Settings and Magma Sources of the Late Cretaceous–Early Paleocene Magmatic Complexes of Northern Kamchatka," Geokhimiya, No. 4, 348–377 (2009) [Geochem. Int. **47**, 329–357 (2009)].
12. A. V. Koloskov, Extended Abstract of Candidate's Dissertation in Geology and Mineralogy (Moscow, 1969).
13. A. V. Koloskov and G. B. Flerov, "Mechanism of Formation and Compositional Features of Hypabyssal Granitoid Massif, Kamchatka," in *Magma of Shallow Chambers* (Nauka, Moscow, 1970), pp. 130–137 [in Russian].
14. A. V. Koloskov and L. V. Zavozina, "Gravity Field in the Exposure Area of Hypabyssal Granitoid Intrusion, Kamchatka," in *Magma of Shallow Chambers* (Nauka, Moscow, 1970), pp. 138–143 [in Russian].
15. A. V. Koloskov, G. B. Flerov, and D. V. Kovalenko, "Late Cretaceous–Paleocene Magmatic Complexes of Central Kamchatka: Geological Settings and Compositional Features," Tikhookean. Geol. **28** (4), 16–34 (2009) [Russ. J. Pac. Geol. **3**, 319–337 (2009)].
16. A. F. Litvinov and N. F. Krikun, *Stage Geological Map of Russian Federation. 1 : 200000. Sheets N-57-XXII, XXVIII, XXIX. Eastern Kamchatka Series* (Izd-vo VSEGEI, St. Petersburg, 1992) [in Russian].
17. M. V. Luchitskaya, A. V. Solov'ev, and J. K. Hourigan, "Two Stages of Granite Formation in the Sredinny Range, Kamchatka: Tectonic and Geodynamic Setting of Granitic Rocks," Geotektonika, No. 4, 49–69 (2008) [Geotectonics **42**, 286–304 (2008)].
18. *Optical and Petrochemical Studies of the Magmatic Complexes of Central Kamchatka*, Ed. by K. N. Rudich (Nauka, Moscow, 1967) [in Russian].
19. K. V. Prokhorov, *Tertiary Granitoids of Kamchatka* (Nauka, Moscow, 1964) [in Russian].
20. Yu. M. Puzankov, "Rare-Metal Volcanic Rocks of the Koryak Highland: Geochemistry, Tectonic Position,

and Genesis," in *Proceedings of Conference on Tectonics, Energetic, and Mineral Resources of Northwestern Pacific* (Khabarovsk, 1989), pp. 50–51 [in Russian].

21. A. V. Solov'ev, *Study of Tectonic Processes in the Areas of Convergent Lithospheric Plates: Methods of Track and Structural Analysis* (Nauka, Moscow, 2008) [in Russian].
22. P. I. Fedorov, D. V. Kovalenko, T. B. Bayanova, and P. A. Serov, "Early Cenozoic Magmatism in the Continental Margin of Kamchatka," Petrologiya **16** (3), 277–295 (2008) [Petrology **16**, 261–278 (2008)].
23. *Formations and Facies of the Upper Cretaceous and Cenozoic Magmatic Complexes of Central Kamchatka*, Ed. by M. A. Favorskaya (Nauka, Moscow, 1968) [in Russian].
24. M. Yu. Khotin, V. I. Vinogradov, O. N. Volynets, et al., "Strontium Isotopic Composition in the Anorthite-Bearing Inclusions in the Kamchatka Volcanics and Basement Rocks," Dokl. Akad. Nauk SSSR **271** (5), 1222–1225 (1993).
25. N. V. Tsukanov, S. G. Skolotnev, and D. P. Savel'ev, "New Evidence for the Composition and Structure of Volcanic Complexes on Cape Nalycheva and the Shipunskii Peninsula, Kamchatka," Vulkanol. Seismol., No. 1, 25–35 (2009) [J. Volcanol. Seismol. **3**, 18–26 (2009)].
26. A. E. Shantser, M. N. Shapiro, A. V. Koloskov, et al., "Structural Evolution of the Lesnovsky Uplift and Its Framing in Cenozoic, Northern Kamchatka," Tikhookean. Geol., No. 4, 66–74 (1985).
27. L. N. Sharpenok, A. E. Kostin, and E. A. Kukharenko, "On Possible Use of Classification TAS Diagram for Diagnostics of the Plutonic Rocks," in *Proceedings of 125th Anniversary Zavaritsky Conference on Magmatism and Ore Formation*, Ed. by N. S. Bortnikov and O. A. Bogatikov, (IGEM RAS, Moscow, 2009), pp. 147–151 [in Russian].
28. B. R. Frost, C. G. Barnes, W. J. Collins, et al., "A Geochemical Classification for Granitic Rocks," J. Petrol. **42** (11), 2033–2048 (2001).
29. J. A. Pearce, N. B. W. Harris, and A. G. Tindle, "Trace Element Discrimination Diagrams for the Tectonic Interpretation of Granitic Rocks," J. Petrol. **25**, 956–983 (1984).
30. R. H. Steiger and E. Jager, "Subcommission on Geochronology: Convention on the Use of Decay Constants in Geo- and Cosmochronology," Earth Planet. Sci. Lett. **36** (3), 359–362 (1977).
31. S. S. Sun and W. F. McDonougt, "Chemical and Isotopic Systematics of Oceanic Basalts: Implications for Mantle Composition and Processes," in *Magmatism in the Ocean Basin*, Ed. by A. D. Saunders and M. I. Norry, Geol. Soc. Spec. Publ. **42**, 313–345 (1989).
32. P. J. Sylvester, "Post-Collisional Strongly Peraluminous Granites," Lithos **45**, 29–44 (1998).
33. V. I. Vinogradov, "Isotopic Evidence of the Conversion of Oceanic Crust To Continental Crust in the Continent-Ocean Transition Zone of Kamchatka," Geochem. Int. **32** (3), 70–109 (1995).

Recommended for publishing by V.G. Sakhno